Spin Hall effect of a light beam in anisotropic metamaterials*

Tang Ming(唐 明), Zhou Xin-Xing(周新星), Luo Hai-Lu(罗海陆)†, and Wen Shuang-Chun(文双春)

Key Laboratory for Micro-/Nano-Optoelectronic Devices of Ministry of Education, School of Information Science and Engineering, Hunan University, Changsha 410082, *China*

(Received 15 May 2012; revised manuscript received 20 July 2012)

We theoretically investigate a switchable spin Hall effect of light (SHEL) in reflection for three specific dispersion relations at an air-anisotropic metamaterial interface. The displacements of horizontal and vertical polarization components vary with the incident angle at different dispersion relations. The transverse displacements can be obtained with the relevant metamaterial whose refractive index can be arbitrarily tailed. The results of the SHEL in the metamaterial provide a new way for manipulating the transverse displacements of a specific polarization component.

Keywords: spin Hall effect of light, metamaterials, horizontal polarization, vertical polarization

PACS: 42.25.–p, 42.79.–e, 41.20.Jb, 78.20.Ci **DOI:** 10.1088/1674-1056/32/12/124201

1. Introduction

The spin Hall effect of light (SHEL) is the photonic version of the spin Hall effect in electronic systems,[1−3] in which the spin photons play the role of spin charge, and a refractive index gradient plays the role of the electric potential gradient.[4−6] Such a spatial gradient of refractive index could occur at an interface between two materials. The SHEL manifests itself as a spin-dependent shift of the beam centroid perpendicular to the refractive index gradient when photons pass through the interface. The SHEL appears as a very small but detectable polarization-dependent displacement perpendicular to the plane of incidence relative to the position predicted by geometrical optics.

The SHEL was first proposed by Onoda *et al.* in 2004.[4] Subsequently, Bliokh *et al.* investigated the SHEL in detail,[5,7] where the SHEL could be considered as a result of the total angular momentum conservation of photons. More recently, there has been a keen interest in the SHEL both in theory[8−15] and experiment.[7,16−21] It is well known to us that the electrodynamic properties of anisotropic materials are significantly different from those of isotropic materials. The anisotropic metamaterial does not require that all the elements of the permittivity and permeability tensors are negative. And the studies of such anisotropic metamaterials have received much attention due to their unusual properties.[22−29] The electromagnetic plane waves propagating in the conventional anisotropic medium exhibit spherical or ellipsoidal wave-vector surfaces.[30,31] In the anisotropic metamaterial, however, the electromagnetic plane wave can exhibit a new hyperboloidal wave-vector surface.[22,23,32] As a result, some new wave propagation characteristics appear. Because of the importance in achieving some potential applications, we will focus our attention on an anisotropic metamaterial whose refractive index can be arbitrarily tailored. It is now possible to obtain a metamaterial whose permittivity and permeability can be varied independently and arbitrarily.[33]

In this work, we explore the SHEL by considering the reflection at an air-anisotropic metamaterial interface for different dispersion relations. First, we establish a general diagram of a propagation model describing the beam reflection at the interface and derive the Fresnel reflection coefficients for horizontal and vertical components. Next, we reveal how the SHEL affects the transverse displacements for three specific dispersion relations. Then, we examine the amplifying displacements and the field distributions for different incident angles. These provide us with a new way to manipulate the SHEL in the anisotropic metamaterial.

*Project supported by the National Natural Science Foundation of China (Grants Nos. 61025024 and 11074068).

†Corresponding author. E-mail: hailuluo@hnu.edu.cn

© 2012 Chinese Physical Society and IOP Publishing Ltd

2. Theoretical analysis

In this section, we give a brief description of the propagation characteristic of an electromagnetic wave in uniaxially anisotropic metamaterials. For anisotropic materials, one or both of the permittivity and permeability are second-rank tensors.[34] In the following, we assume that both the permittivity and permeability are uniaxially anisotropic. For an uniaxially anisotropic medium, if we take the optical axis as the z axis, the permittivity and permeability tensors will have the following forms according to Ref. [35]:

$$\epsilon = \begin{pmatrix} \epsilon_\perp & 0 & 0 \\ 0 & \epsilon_\perp & 0 \\ 0 & 0 & \epsilon_\parallel \end{pmatrix}, \quad \mu = \begin{pmatrix} \mu_\perp & 0 & 0 \\ 0 & \mu_\perp & 0 \\ 0 & 0 & \mu_\parallel \end{pmatrix}, \tag{1}$$

where $\epsilon_\parallel$, $\mu_\parallel$ and $\epsilon_\perp$, $\mu_\perp$ are the permittivity and permeability constants in the directions parallel and perpendicular to the optical axis, respectively.

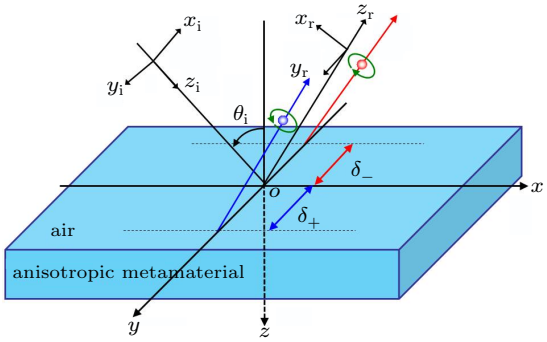


Fig. 1. (color online) Schematic diagram of SHEL at an air-anisotropic metamaterial interface, where θ_i is the incident angle; $\delta_\pm$ are the displacements of right-circularly and left-circularly polarized spin components. Subscripts i and r represent incident and reflected light, respectively.

We will discuss the SHEL of the reflection of light passing from one isotropic right-handed material into a second uniaxially anisotropic metamaterial, the optical axis of the anisotropic metamaterial is normal to the interface of the two media, which is shown in Fig. 1. In the following, we will denote the permittivity and permeability of the isotropic right-handed medium as ϵ_r and μ_r, respectively. The permittivity and permeability tensors of the metamaterial have been given in Eqs. (1) and (2). Since the system is isotropic in the x–y plane, we can assume that the isotropic right-handed material is the top of the x–y plane and the wave vectors of the incident and the reflected fields are in the x–z plane without lose of generality. Consider the propagation of a plane wave of angular frequency ω with $\boldsymbol{E} = \boldsymbol{E}_0 \exp(\mathrm{i}\boldsymbol{k}\cdot\boldsymbol{r} - \mathrm{i}\omega t)$ and $\boldsymbol{H} = \boldsymbol{H}_0 \exp(\mathrm{i}\boldsymbol{k}\cdot\boldsymbol{r} - \mathrm{i}\omega t)$ from an isotropic right-handed material into an anisotropic metamaterial. The field can be described by Maxwell's equations

$$\boldsymbol{\nabla}\times\boldsymbol{E} = -\frac{\partial \boldsymbol{B}}{\partial t}, \quad \boldsymbol{B} = \mu_0\boldsymbol{\mu}\boldsymbol{H}, \tag{2}$$

$$\boldsymbol{\nabla}\times\boldsymbol{H} = \frac{\partial \boldsymbol{D}}{\partial t}, \quad \boldsymbol{D} = \epsilon_0\boldsymbol{\epsilon}\boldsymbol{E}. \tag{3}$$

For the plane waves in the isotropic right-handed material, Maxwell's equations yield the corresponding dispersion relation in the familiar form

$$k_x^2 + k_y^2 + k_z^2 = \frac{\omega^2}{c^2}, \tag{4}$$

where k_i is the i-th component of the incident wave vector in the isotropic right-handed material, and c is the speed of light in vacuum. We can obtain the dispersion relations in the anisotropic medium with a more careful calculation of Maxwell's equations[36]

$$\frac{q_x^2}{\epsilon_\perp\mu_{||}} + \frac{q_y^2}{\epsilon_\perp\mu_{||}} + \frac{q_z^2}{\epsilon_\perp\mu_\perp} = \frac{\omega^2}{c^2}, \tag{5}$$

$$\frac{q_x^2}{\epsilon_\parallel\mu_\perp} + \frac{q_y^2}{\epsilon_\parallel\mu_\perp} + \frac{q_z^2}{\epsilon_\perp\mu_\perp} = \frac{\omega^2}{c^2}, \tag{6}$$

where q_i represents the i-th component of the wave vector in the anisotropic metamaterial. The above equation can be represented by a three-dimensional surface in the wave-vector space. This surface is known as the normal surface and consists of two shells. It can be easily shown that there are two types of linearly polarized plane waves in Eqs. (5) and (6), namely vertical polarized and horizontal polarized plane waves.[36]

We can easily obtain the Fresnel reflection coefficients according to the corresponding boundary conditions and Maxwell's equations. For the vertical polarized plane wave component, the reflection coefficient can be expressed as

$$r_\mathrm{s} = \frac{k_z\epsilon_\perp - q_z\epsilon_\mathrm{r}}{k_z\epsilon_\perp + q_z\epsilon_\mathrm{r}}. \tag{7}$$

Similarly, we can obtain the reflection coefficient for the horizontal polarized plane wave component

$$r_\mathrm{p} = \frac{k_z\mu_\perp - q_z\mu_\mathrm{r}}{k_z\mu_\perp + q_z\mu_\mathrm{r}}. \tag{8}$$

Here, we investigate the spin-dependent transverse displacements of the reflected light induced by the SHEL. At any given plane $z_\mathrm{a} = \text{const.}$, the transverse displacement of field centroid compared to the geometrical-optics prediction is given by

$$\delta_\pm = \frac{\iint y_\mathrm{r} I_\pm(x_\mathrm{r}, y_\mathrm{r}, z_\mathrm{r})\,\mathrm{d}x_\mathrm{r}\,\mathrm{d}y_\mathrm{r}}{\iint I_\pm(x_\mathrm{r}, y_\mathrm{r}, z_\mathrm{r})\,\mathrm{d}x_\mathrm{r}\,\mathrm{d}y_\mathrm{r}}. \tag{9}$$

The intensity distribution of beam is closely linked to the longitudinal momentum current $I(x_\mathrm{r}, y_\mathrm{r}, z_\mathrm{r}) \propto \boldsymbol{P}_\mathrm{r}\cdot\boldsymbol{e}_{\mathrm{r}z}$. The time-averaged linear momentum density associated with the electromagnetic field can be shown to be $\boldsymbol{P}_\mathrm{r} \propto \mathrm{Re}[\boldsymbol{E}_\mathrm{r}\times\boldsymbol{H}_\mathrm{r}^*]$, where the magnetic field can be obtained by $\boldsymbol{H}_\mathrm{r} = -\mathrm{i}k_\mathrm{r}^{-1}\boldsymbol{\nabla}\times\boldsymbol{E}_\mathrm{r}$.[6]

We then explore the spin-dependent transverse displacement of the reflected field. Our analysis shows that the magnitude of the splitting between the two spin components of the reflected light depends on the particular polarization state of the incident light[37]

$$\delta_{\pm}^{\mathrm{H}} = \mp\frac{\lambda}{2\pi}[1 + (|r_{\mathrm{s}}|/|r_{\mathrm{p}}|)\cos(\varphi_{\mathrm{s}} - \varphi_{\mathrm{p}})]\cot\theta_i, \quad (10)$$

$$\delta_{\pm}^{\mathrm{V}} = \mp\frac{\lambda}{2\pi}[1 + (|r_{\mathrm{p}}|/|r_{\mathrm{s}}|)\cos(\varphi_{\mathrm{s}} - \varphi_{\mathrm{p}})]\cot\theta_i. \quad (11)$$

where $r_{\mathrm{p,s}} = |r_{\mathrm{p,s}}|\exp(\mathrm{i}\varphi_{\mathrm{p,s}})$. Note that these expressions are slightly different from those in the previous work,[37,38] since the Fresnel reflection coefficients are no longer always real in some cases.

3. Spin Hall effect of light

We will explore the SHEL at the air–metamaterial interface for three specific dispersion relations, as shown in Fig. 2. How to enhance or suppress the transverse displacement in SHEL is of interest to us. The metamaterial whose refractive index can be tailored arbitrarily may become a good candidate for manipulating the SHEL. The refractive index of metamaterial can be designed by rationally choosing its parameters. Different parameters lead to different types of dispersion relations. It should be noted that for the same dispersion relation, there exist two subtypes of wavevector surfaces which can be formed from the combinations of tensor elements. In fact, the two subtypes can be discussed in a similar way. Hence we do not need to discuss every subtype in detail. We proceed to examine the role of dispersion relation in the SHEL. In order to better study the influence of the dispersion relation on the SHEL, we set the refractive index of YVO_4 as the reference object. The refractive index for the ordinary and the extraordinary rays at 632.8 nm are $n_{\mathrm{o}} = 1.992$ and $n_{\mathrm{e}} = 2.218$, respectively.

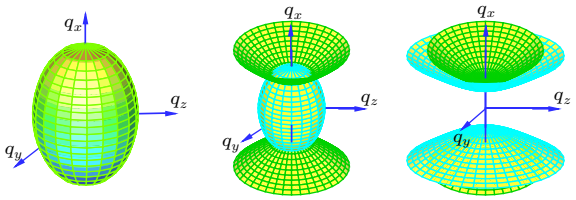


Fig. 2. (color online) (a) Both horizontal and vertical polarized waves have the ellipsoid dispersion relations. (b) The horizontal polarized waves have the ellipsoid dispersion relation, while the vertical polarized waves have the hyperboloid dispersion relation. (c) Both horizontal and vertical polarized waves have the hyperboloid dispersion relations.

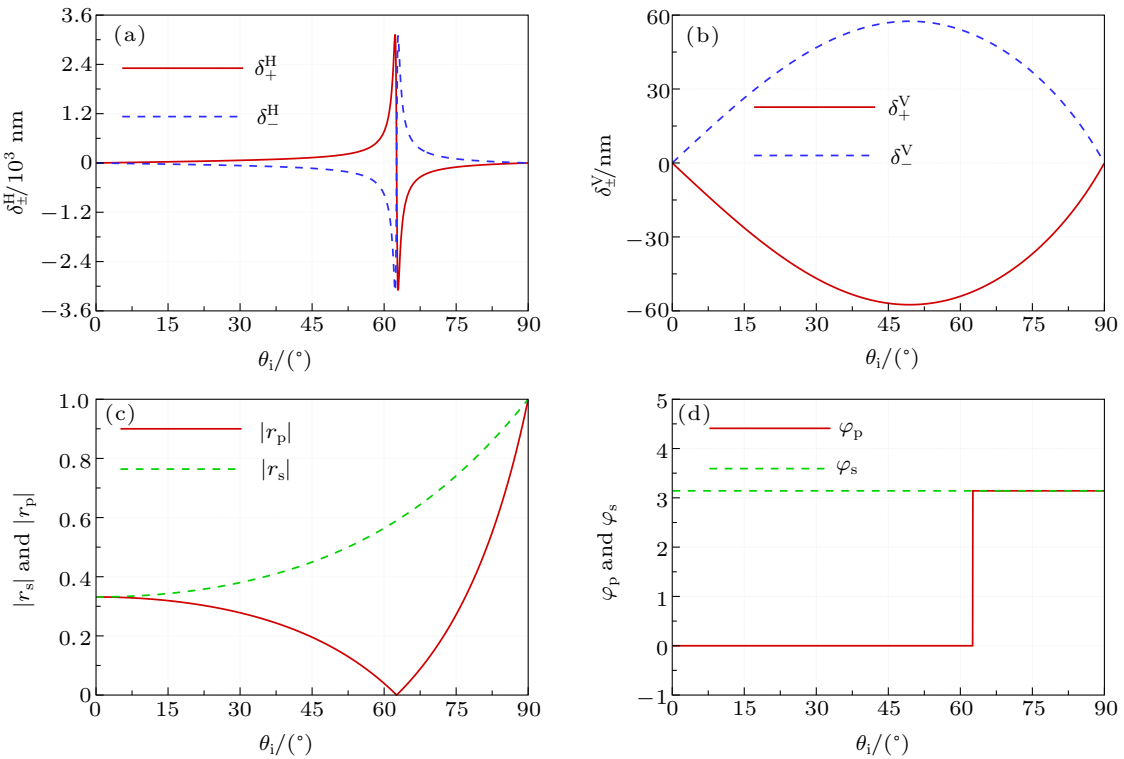


Fig. 3. (color online) (a) The displacement $\delta_{\pm}^{\mathrm{H}}$ of the spin polarized component as a function of the incident angle in the case of horizontal polarization. (b) The displacement $\delta_{\pm}^{\mathrm{V}}$ of the spin polarized component as a function of the incident angle in the case of vertical polarization. (c) Fresnel reflection coefficients r_{s} and r_{p} each as a function of the incident angle. (d) The phases of Fresnel reflection coefficients r_{s} and r_{p} each as a function of the incident angle.

If $\mu_\perp$, $\epsilon_\perp$, $\mu_\parallel$, and $\epsilon_\parallel$ are positive, both horizontal and vertical polarized waves have the ellipsoid dispersion relation. Let $\mu_\perp = \mu_\parallel = 1$, $\epsilon_\perp = n_o^2 = 3.97$, $\epsilon_\parallel = n_e^2 = 4.92$. Figure 3 describes the displacements $\delta_\pm^H$ and $\delta_\pm^V$ of the spin polarized components induced by SHEL each as a function of the incident angle in the cases of horizontal polarization and vertical polarization.

The displacement of the horizontal polarization component increases with the increasing θ_i and reaches a maximum (3200 nm) near the Brewster angle, then changes rapidly when approaching the Brewster angle $\theta_B = 62.6°$. When $\theta_i > \theta_B$, the displacement decreases with the increasing θ_i, as shown in Fig. 3(a). The displacement of the vertical polarization component increases and reaches the maximum (57 nm), then subsequently decreases to zero as the incident angle increases from 0° to 90°, as shown in Fig. 3(b). We find that the transverse displacement of the horizontal polarization component is much larger than that of the vertical polarization component. From Eqs. (10) and (11), we know that the transverse displacements of horizontal and vertical polarizations would have different tendencies for the increasing incident angle. Fresnel reflection coefficients $|r_s|$ and $|r_p|$ versus the incident angle are shown in Fig. 3(c). It is obvious that $(|r_s|/|r_p|)\cos(\varphi_s - \varphi_p)$ and $(|r_p|/|r_s|)\cos(\varphi_p - \varphi_s)$ in Eqs. (10) and (11) determine the magnitudes of the transverse displacements of the wave-packet centroid since the other quantities in the two equations are constant. The φ_p and φ_s versus the incident angle shown in Fig. 3(d) indicates that $|\cos(\varphi_s - \varphi_p)| = 1$ and the magnitude of $\delta_\pm$ only depends on $|r_s|/|r_p|$ or $|r_p|/|r_s|$ for a given incident angle. At the Brewster angle θ_B, the ratio of Fresnel reflection coefficients r_s and r_p reaches the maximum. Therefore, the transverse displacement of the horizontal polarization component is huge at the Brewster angel. Figure 4 describes the amplifying displacements $\delta_\omega = A_\omega \delta_+^H$ versus the incident angle θ_i and the field distributions at different incident angles. When $\theta_i = \theta_B = 62.6°$, the field distribution is completely symmetrical. When $\theta_i > \theta_B$ (62.6°), the field distribution shifts upwards. When $\theta_i < \theta_B$ (61.6°), the field distribution shifts downwards. These agree with the principle of weak measurements and our early results.[6]

If $\mu_\perp$, $\epsilon_\parallel$, and $\epsilon_\perp$ are positive, $\mu_\parallel$ is negative, the horizontal polarized waves have the ellipsoid dispersion relation, and the vertical polarized waves have the hyperboloid dispersion relation. Let $\mu_\perp = 1, \mu_\parallel = -1$, $\epsilon_\perp = 3.97$, $\epsilon_\parallel = 4.92$. Figure 5 describes the displacements of horizontal and vertical polarization components induced by the SHEL. Figure 6 describes the amplifying displacement δ_ω as a function of the incident angle θ_i and the field distributions at different incident angles. The change trends are the same as those in Figs. 3(a), 3(b), and 4. However, the Brewster angle is different, and in this case $\theta_B = 57.5°$. The maximum of the displacement of the horizontal polarization component is 4200 nm, which is larger than 3200 nm in Fig. 3(a). And the maximum of the displacement of the vertical polarization component is 71.4 nm. We also find that the transverse displacement of the horizontal polarization component is much larger than that of the vertical polarization component, which is due to the same reason as that in the case of Figs. 3(a) and 3(b). It is interesting to note that the transverse displacements are in the range of negative-zero-positive values for the horizontal polarization, which can be modulated via tuning the incident angle (Figs. 3(a) and 5(a)). It indicates that the SHEL can be greatly enhanced or suppressed, or even completely eliminated.

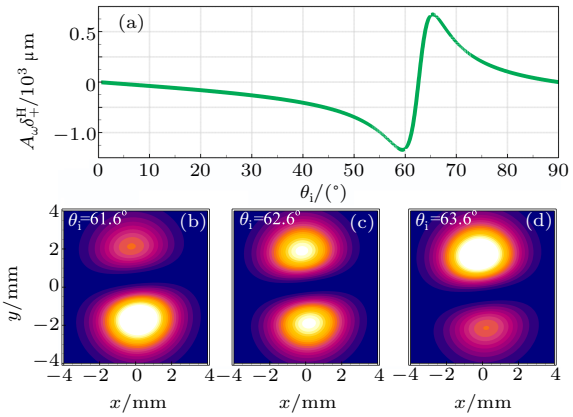


Fig. 4. (color online) (a) The amplifying displacements δ_ω as a function of the incident angle. (b) The field distributions at (b) $\theta_i = 61.6°$, (c) $\theta_i = 62.6°$, and (d) $\theta_i = 63.6°$.

If $\mu_\perp$ and $\epsilon_\parallel$ are negative, $\mu_\parallel$ and $\epsilon_\perp$ are positive, both horizontal and vertical polarized waves have the hyperboloid dispersion relation. Let $\mu_\perp = -1$, $\mu_\parallel = 1$, $\epsilon_\perp = 3.97$, $\epsilon_\parallel = -4.92$. Figure 7 describes the displacements of horizontal and vertical polarization components induced by the SHEL. The displacements of horizontal and vertical polarization components are almost the same in this case. They increase with the increasing θ_i and reach 30 nm, then approach to zero as the incident angle increases from 0° to 90°, as shown in Figs. 7(a) and 7(b). It is found that the total reflection occurs at the air–metamaterial interface and the Fresnel reflection coefficients are no longer real. The Fresnel reflection coefficients and the phases of reflection coefficients are shown in Figs. 7(c)

and 7(d), respectively. Figure 8 describes the amplifying displacement δ_ω as a function of the incident angle θ_i and the field distributions at different incident angles. Due to the total reflection, the Fresnel reflection coefficients are $|r_s| = |r_p| = 1$, and the transverse displacements depend on the incident angle and the phases of Fresnel reflection coefficients φ_p and φ_s. The field distributions and the amplifying displacements are completely different from those in Figs. 4 and 6. We can obtain the same transverse displacement for the horizontal and the vertical polarization components in this case by adjusting the incident angle.

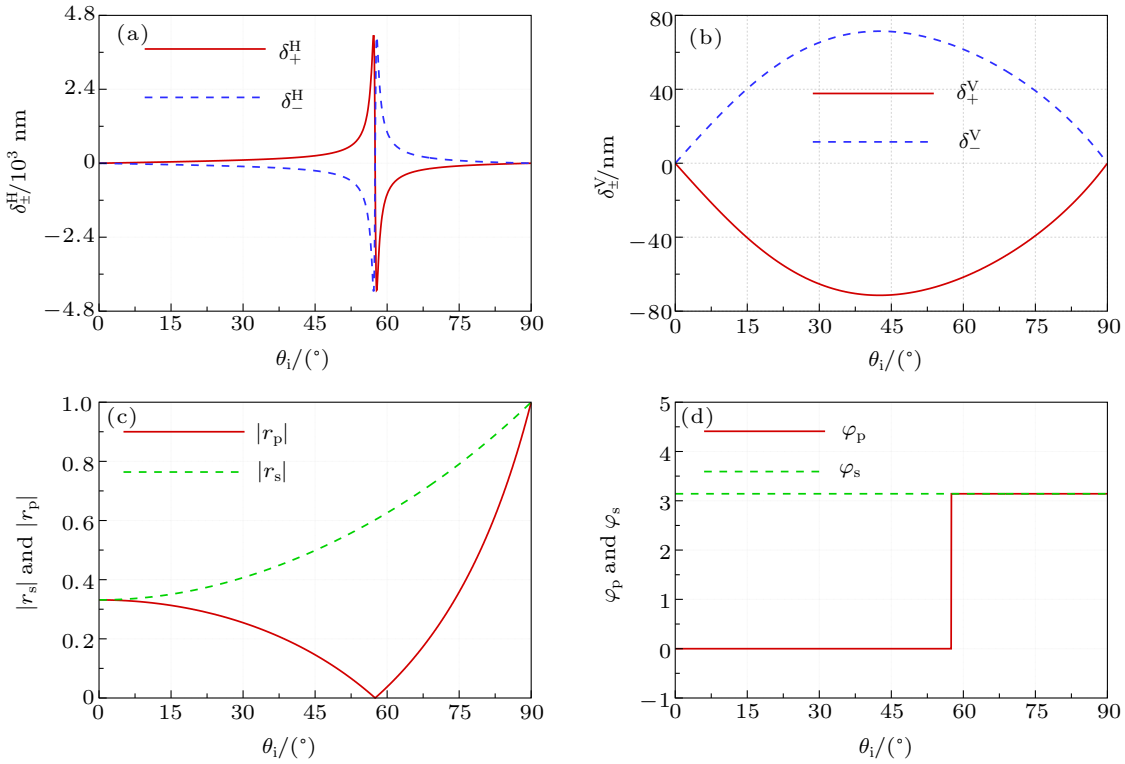


Fig. 5. (color online) (a) The displacement $\delta_\pm^H$ of the spin polarized component as a function of the incident angle in the case of horizontal polarization. (b) The displacement $\delta_\pm^V$ of the spin polarized component as a function of the incident angle in the case of vertical polarization. (c) Fresnel reflection coefficients r_s and r_p each as a function of the incident angle. (d) The phases of Fresnel reflection coefficients r_s and r_p each as a function of the incident angle.

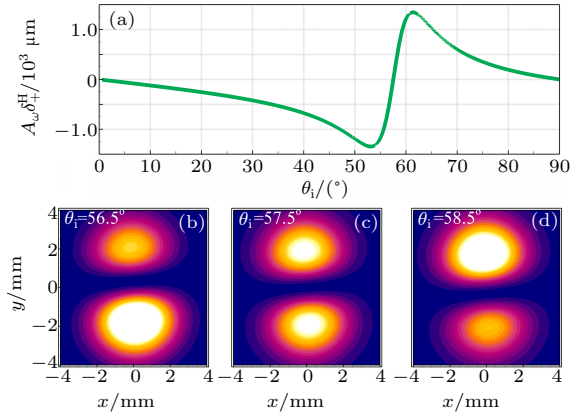


Fig. 6. (color online) (a) The amplifying displacement δ_ω as a function of the incident angle. (b) The field distributions at (b) $\theta_i = 56.5^\circ$, (c) $\theta_i = 57.5^\circ$, and (d) $\theta_i = 58.5^\circ$.

From the above analysis, the transverse displacements of the horizontal polarization component are very large near the Brewster angle and can be tuned to either a negative or a positive value, or even to zero, by just adjusting the incident angle, as shown in Figs. 3(a) and 5(a). However, the transverse displacements of the vertical polarization component are much smaller than those of the horizontal polarization component, as shown in Figs. 3(b) and 5(b). Furthermore, the transverse displacements of horizontal and vertical polarization components are the same in the case of total reflection, as shown Figs. 7(a) and 7(b). The above results show that the transverse displacements of horizontal and vertical polarization components are closely interrelated with the values of $\mu_\perp$, $\mu_\parallel$, $\epsilon_\perp$, $\epsilon_\parallel$, and θ_i. We can obtain huge transverse displacements of horizontal and vertical polarization components in the case of different dispersion relations.

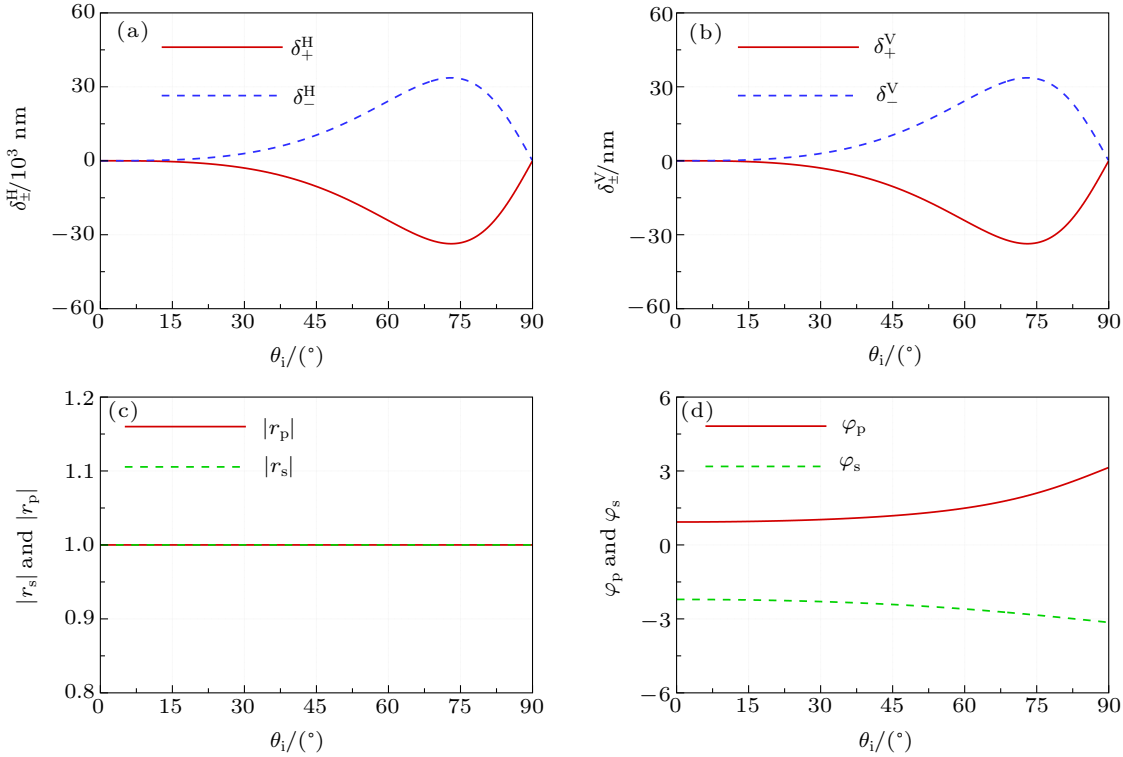


Fig. 7. (color online) (a) The displacement $\delta_{\pm}^{H}$ of the spin-polarized component as a function of the incident angle in the case of horizontal polarization. (b) The displacement $\delta_{\pm}^{V}$ of the spin-polarized component as a function of the incident angle in the case of vertical polarization. (c) Fresnel reflection coefficients r_s and r_p each as a function of the incident angle. (d) The phases of Fresnel reflection coefficients r_s and r_p each as a function of the incident angle.

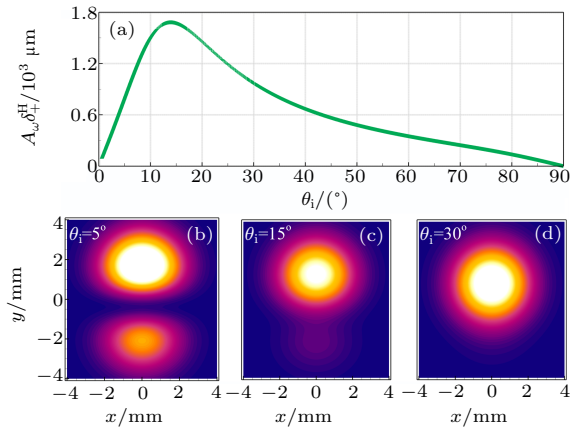


Fig. 8. (color online) (a) The amplifying displacement δ_ω as a function of the incident angle. The field distributions at (b) $\theta_i = 5°$, (c) $\theta_i = 15°$, and (d) $\theta_i = 30°$.

4. Conclusion

In conclusion, we have presented a theoretical research on the tunable SHEL for horizontal and vertical polarization components at an air-anisotropic metamaterial interface. If $\mu_\perp$, $\epsilon_\perp$, $\mu_\parallel$, and $\epsilon_\parallel$ are positive, or $\mu_\perp$, $\epsilon_\parallel$, and $\epsilon_\perp$ are positive, $\mu_\parallel$ is negative, the transverse displacements of horizontal polarization can be amplified and switched near the Brewster angle, which is in the range of negative-zero-positive values and can be modulated via tuning the incident angle. If $\mu_\perp$ and $\epsilon_\parallel$ are negative, $\mu_\parallel$ and $\epsilon_\perp$ are positive, the transverse displacements of horizontal and vertical polarizations are the same due to the total reflection. Therefore, the transverse displacements of horizontal and vertical polarization components can be switched by adjusting the incident angle. It is expected that the SHEL in the anisotropic metamaterial whose refractive index can be tailored arbitrarily will be useful for nano-photonic devices.

References

[1] Sinova J, Culcer D, Niu Q, Sinitsyn N A, Jungwirth T and MacDonald A H 2004 *Phys. Rev. Lett.* **92** 126603
[2] Murakami S, Nagaosa N and Zhang S C 2003 *Science* **301** 1348
[3] Wunderlich J, Kaestner B, Sinova J and Jungwirth T 2005 *Phys. Rev. Lett.* **94** 047204
[4] Onoda M, Murakami S and Nagaosa N 2004 *Phys. Rev. Lett.* **93** 083901
[5] Bliokh K Y and Bliokh Y P 2006 *Phys. Rev. Lett.* **96** 073903

[6] Luo H, Zhou X, Wen S, Shu W and Fan D 2011 *Phys. Rev.* A **84** 043806

[7] Bliokh K Y, Niv A, Kleiner V and Hasman E 2008 *Nat. Photon.* **2** 748

[8] Gosselin P, Bérard A and Mohrbach H 2007 *Phys. Rev.* D **75** 084035

[9] Aiello A and Woerdman J P 2008 *Opt. Lett.* **33** 1437

[10] Aiello A, Lindlein N, Marquardt C and Leuchs G 2009 *Phys. Rev. Lett.* **103** 100401

[11] Luo H, Wen S, Shu W, Tang Z, Zou Y and Fan D 2009 *Phys. Rev.* A **80** 043810

[12] Ma J, Luo H L and Wen S C 2011 *Acta Phys. Sin.* **60** 094205 (in Chinese)

[13] Liu S, Luo H L and Wen S C 2011 *Acta Phys. Sin.* **60** 074208 (in Chinese)

[14] Luo X, Zhou X X, Luo H L and Wen S C 2012 *Acta Phys. Sin.* **61** 194202 (in Chinese)

[15] Ling X H, Luo H L, Tang M and Wen S C 2012 *Chin. Phys. Lett.* **29** 074209

[16] Haefner D, Sukhov S and Dogariu A 2009 *Phys. Rev. Lett.* **102** 123903

[17] Rodríguez-Herrera O G, Lara D, Bliokh K Y, Ostrovskaya E A and Dainty C 2010 *Phys. Rev. Lett.* **104** 253601

[18] Qin Y, Li Y, Feng X, Liu Z, He H, Xiao Y and Gong Q 2010 *Opt. Express* **18** 16832

[19] Ménard J, Mattacchione A E, Vandriel Hautmann H M C and Betz M 2010 *Phys. Rev.* B **82** 045303

[20] Luo H, Ling X, Shu W, Wen S and Fan D 2011 *Phys. Rev.* B **84** 033801

[21] Zhou X, Xiao Z, Luo H and Wen S 2012 *Phys. Rev.* A **85** 043809

[22] Hu L and Chui S T 2002 *Phys. Rev.* B **66** 085108

[23] Smith D R and Schurig D 2003 *Phys. Rev. Lett.* **90** 077405

[24] Zhou L, Chan C T and Sheng P 2003 *Phys. Rev.* B **68** 115424

[25] Luo H, Hu W, Yi X, Liu H and Zhu J 2005 *Opt. Commun.* **254** 353

[26] Shen N H, Wang Q, Chen J, Fan Y X, Ding J, Wang H T, Tian Y and Ming N B 2005 *Phys. Rev.* B **72** 153104

[27] Luo H, Shu W, Li F and Ren Z 2006 *Opt. Commun.* **267** 271

[28] Luo H, Hu W, Shu W, Li F and Ren Z 2006 *Europhys. Lett.* **74** 1081

[29] Yi X L, Liu J S, Chen H and Du Q J 2010 *Chin. Phys.* B **19** 114204

[30] Yariv A and Yeh P 1984 *Optical Waves in Crystals* (New York: Wiley)

[31] Born M and Wolf E 1999 *Principles of Optics* (New York: Cambridge University Press)

[32] Lindell I V, Tretyakov S A, Nikoskinen K I and Ilvonen S 2001 *Microw. Opt. Technol. Lett.* **31** 129

[33] Pendry J, Schurig D and Smith D 2006 *Science* **312** 1780

[34] Lanndau and Lifshitz E M 1960 *Electrodynamics of Continuous Media* (New York: Pergamon) Chap. 11

[35] Pochi Y 1979 *J. Opt. Soc. Am.* **69** 742

[36] Luo H, Ren Z, Shu W and Li F 2007 *Appl. Phys.* A **87** 245

[37] Hosten O and Kwiat P 2008 *Science* **319** 787

[38] Qin Y, Li Y, He H Y and Gong Q H 2009 *Opt. Lett.* **34** 2551